

1972

A finite element method for calculating stress intensity factors and its application to composites

Spiros George Papaioannou
Lehigh University

Follow this and additional works at: <https://preserve.lehigh.edu/etd>



Part of the [Mechanical Engineering Commons](#)

Recommended Citation

Papaioannou, Spiros George, "A finite element method for calculating stress intensity factors and its application to composites" (1972).
Theses and Dissertations. 4046.
<https://preserve.lehigh.edu/etd/4046>

This Thesis is brought to you for free and open access by Lehigh Preserve. It has been accepted for inclusion in Theses and Dissertations by an authorized administrator of Lehigh Preserve. For more information, please contact preserve@lehigh.edu.

A FINITE ELEMENT METHOD FOR CALCULATING
STRESS INTENSITY FACTORS AND ITS
APPLICATION TO COMPOSITES

by Spiros George Papaioannou

ABSTRACT

A concept which allows the development of efficient finite element techniques for the analysis of plane elastic structures containing cracks is discussed. It consists in combining a special finite element covering a small area around each crack tip, with conventional CST elements in the rest of the region. For the special element a pair of displacement functions is chosen, which adequately represents the singular character of the elastic solution at the tip.

The application of this concept is illustrated through a specific numerical method developed by W. K. Wilson for the calculation of mode I stress intensity factors.

Wilson's method was coded and used to analyze an infinitely long strip under tension with a line crack perpendicular to its axis of symmetry. Circular inclusions of different material properties were assumed to be present near the tips of the crack and their effect on the mode I stress intensity factor was investigated.

It was found that more flexible inclusions increase the intensity factor while more rigid inclusions decrease it. These results are quite similar to those obtained by analytical methods in an analogous problem involving an infinite sheet, but in the case of a strip, the influence of inclusions on the intensity factor was found to be more pronounced.

A FINITE ELEMENT METHOD FOR CALCULATING
STRESS INTENSITY FACTORS AND ITS
APPLICATION TO COMPOSITES

by

Spiros George Papaioannou

A Thesis

Presented to the Graduate Committee

of Lehigh University

in Candidacy for the Degree of

Master of Science

in

Mechanical Engineering

Lehigh University

1972

This thesis is accepted and approved in partial fulfillment
of the requirements for the degree of Master of Science.

Sept. 13, 1972

(date)

Robert A. Lucas

Professor in Charge

Robert G. Lumbri

Chairman of Department

ACKNOWLEDGMENTS

The work presented in this thesis was carried out under the direction of Professor Robert A. Lucas and the author wishes to express his deep appreciation for this guidance and assistance.

In addition, grateful appreciation is due to Professor Peter D. Hilton for his many useful suggestions.

Finally, the Lehigh University Computing Center which provided the computer facilities is to be thanked for its generous support.

TABLE OF CONTENTS

	Page
ABSTRACT	1
1. INTRODUCTION	3
2. THE METHOD OF FINITE ELEMENTS	5
3. SPECIAL FINITE ELEMENT TECHNIQUES	9
4. WILSON'S METHOD	12
4.1 CONSTRUCTION OF THE TOTAL STIFFNESS MATRIX	15
4.2 MATRIX FORMULATION	19
4.3 DISPLACEMENT OF THE CRACK TIP	22
4.4 CALCULATION OF THE MODE I STRESS INTENSITY FACTOR	23
5. APPLICATION TO A CRACKED STRIP UNDER TENSION	26
5.1 EVALUATION OF THE METHOD'S ACCURACY	30
5.2 INFLUENCE OF INCLUSIONS ON THE INTENSITY FACTOR	31
6. FINAL REMARKS	40
7. COMPUTER PROGRAM	41
BIBLIOGRAPHY	44
BIOGRAPHICAL NOTE	45

LIST OF TABLES

	Page
1. Correction Factor $f(\lambda)$ (equation (50)).	30
2. Stress Intensity Factor K in $\text{psi in}^{1/2}$ versus the Shear Modulus Ratio μ_j/μ for various values of R/a , $b/a=2.0$, $d=25\text{in}$	34
3. Stress Intensity Factor K in $\text{psi in}^{1/2}$ versus the Shear Modulus Ratio μ_j/μ for various values of R/a , $b/a=3.0$, $d=25\text{in}$	35
4. Stress Intensity Factor K in $\text{psi in}^{1/2}$ versus the Shear Modulus Ratio μ_j/μ for various values of R/a , $b/a=4.0$, $d=25\text{in}$	36

LIST OF FIGURES

	Page
1. Infinitely long cracked strip under tension with inclusions	27
2. Finite element layout of one fourth of the strip area	28
3. Typical finite element layout with inclusion	29
4. Element pattern around the crack tip with $r_c = 0.4$ in and $N = 25$	32
5. Element pattern around the crack tip with $r_c = 0.3$ in and $N = 49$	32
6. Normalized Stress Intensity Factor K/K_0 versus the Shear Modulus Ratio μ_j/μ for various values of R/a , $b/a=2.0$, $d=25$ in.	37
7. Normalized Stress Intensity Factor K/K_0 versus the Shear Modulus Ratio μ_j/μ for various values of R/a , $b/a=3.0$, $d=25$ in.	38
8. Normalized Stress Intensity Factor K/K_0 versus the Shear Modulus Ratio μ_j/μ for various values of R/a , $b/a=4.0$, $d=25$ in.	39

LIST OF SYMBOLS

σ_x	stress in x direction
σ_y	stress in y direction
τ_{xy}	shearing stress
u	displacement in x direction
v	displacement in y direction
r, θ	polar coordinates
r_c	radius of the circular crack tip element
K_I	mode I stress intensity factor
K_{II}	mode II stress intensity factor
h	elastic constant, = ν for plane strain, = $\frac{\nu}{1+\nu}$ for plane stress
ν	Poisson's ratio
Π	total potential energy of the whole structure
Π_t	total potential energy of the system of triangular elements
Π_c	total potential energy of the circular crack tip element
$[]^T$	matrix transpose
$[\omega_i]$	displacement vector of node i
$[\omega_t]$	displacement vector of the crack tip

$\delta_1, \delta_2, \delta_3, \delta_4$	circular crack tip (SSC-4) element parameters
$[A] = [a_{ij}]$	stiffness matrix of the circular crack tip element
σ	uniformly distributed external load
μ	shear modulus
μ_i	shear modulus of the inclusion
K	stress intensity factor with inclusion
K_0	stress intensity factor without inclusion

A FINITE ELEMENT METHOD FOR CALCULATING
STRESS INTENSITY FACTORS AND ITS
APPLICATION TO COMPOSITES

by Spiros George Papaioannou

ABSTRACT

A concept which allows the development of efficient finite element techniques for the analysis of plane elastic structures containing cracks is discussed. It consists in combining a special finite element covering a small area around each crack tip, with conventional CST elements in the rest of the region. For the special element a pair of displacement functions is chosen, which adequately represents the singular character of the elastic solution at the tip.

The application of this concept is illustrated through a specific numerical method developed by W. K. Wilson for the calculation of mode I stress intensity factors.

Wilson's method was coded and used to analyze an infinitely long strip under tension with a line crack perpendicular to its axis of symmetry. Circular inclusions of different material properties were assumed to be present near the tips of the crack and their effect on the mode I stress intensity factor was investigated.

It was found that more flexible inclusions increase the intensity factor while more rigid inclusions decrease it. These results are quite similar to those obtained by analytical methods in an analogous problem involving an infinite sheet, but in the case of a strip, the influence of inclusions on the intensity factor was found to be more pronounced.

1. INTRODUCTION

The distribution of stresses in bodies containing cracks is always characterized by stress concentration in the vicinity of each crack tip. In general, the stress field around the tip of a crack has received the utmost attention, since progressive increase in the magnitude of the stresses at this point eventually results in additional growth of the crack and catastrophic material failure.

For plane elasticity loading conditions, the stress field associated with the tip is described by the asymptotic equations

$$\sigma_x = \frac{K_I}{(2\pi r)^{\frac{1}{2}}} \cos \frac{\theta}{2} [1 - \sin \frac{\theta}{2} \sin \frac{3\theta}{2}] - \frac{K_{II}}{(2\pi r)^{\frac{1}{2}}} \sin \frac{\theta}{2} [2 + \cos \frac{\theta}{2} \cos \frac{3\theta}{2}] \quad (1)$$

$$\sigma_y = \frac{K_I}{(2\pi r)^{\frac{1}{2}}} \cos \frac{\theta}{2} [1 + \sin \frac{\theta}{2} \sin \frac{3\theta}{2}] + \frac{K_{II}}{(2\pi r)^{\frac{1}{2}}} \sin \frac{\theta}{2} \cos \frac{\theta}{2} \cos \frac{3\theta}{2} \quad (2)$$

$$\tau_{xy} = \frac{K_I}{(2\pi r)^{\frac{1}{2}}} \sin \frac{\theta}{2} \cos \frac{\theta}{2} \cos \frac{3\theta}{2} + \frac{K_{II}}{(2\pi r)^{\frac{1}{2}}} \cos \frac{\theta}{2} [1 - \sin \frac{\theta}{2} \sin \frac{3\theta}{2}] \quad (3)$$

The term "asymptotic" comes from the fact that these equations become increasingly more accurate as one approaches

the tip.

K_I and K_{II} are the mode I and mode II stress intensity factors. These factors do not depend on the coordinates r and θ and their magnitude is a measure of the intensity of the stress field. Thus, the prediction of strength requires that the stress intensity factors be known and, therefore, considerable effort is currently being devoted to the development of computational techniques for their determination.

Analytical techniques are very important, but they are applicable only to idealized geometries. In many practical situations, as for example the problem of a cracked elastic strip under tension with inclusions examined in this thesis, analytical solutions are very difficult or even impossible to obtain. For these problems numerical techniques are increasingly being used, because of their ability to treat quite general geometric and loading conditions. These techniques are almost invariably based on the method of finite elements.

2. THE METHOD OF FINITE ELEMENTS

Since most numerical techniques for the computation of stress intensity factors are essentially variations of the method of finite elements, a brief description of this basic method is necessary. A more detailed discussion of the method can be found in reference [1].

The two-dimensional continuum is divided by imaginary lines into a number of "finite elements". Usually these elements are triangular but many other shapes are possible and may be found useful for special purposes.

The elements are assumed to be interconnected at a discrete number of nodes located on their boundaries. In the case of triangular elements, the nodes coincide with the corners of the triangles.

Within each element, a pair of displacement functions is chosen, defining the displacement components u, v at each point, in terms of the displacements at the nodal points of the element.

Through the displacement functions, the state of strain within each element is uniquely defined. Since the elastic properties of the material are assumed to be known, the state of stress is also defined.

The principle of minimum potential energy can then be expressed in mathematical form and this leads to a system of simultaneous equations

$$\frac{\partial \Pi}{\partial [\omega_i]} = 0 \quad i=1, \dots, n \quad (4)$$

These equations finally assume the form

$$\frac{\partial \Pi}{\partial [\omega_i]} = \sum \frac{\partial \Pi_e}{\partial [\omega_i]} - [R_i] = 0 \quad i=1, \dots, n \quad (5)$$

where Π_e is the potential energy of each element e

$[R_i]$ is the external load vector acting on node i

$$\frac{\partial \Pi_e}{\partial [\omega_i]} = \frac{\partial [\omega_e]}{\partial [\omega_i]} ([K_e][\omega_e] - [R_e]) \quad (6)$$

$[\omega_e] = [u_i v_i u_j v_j \dots u_m v_m]^T$ i, j, \dots, m the nodal points of element e

$$[K_e] = \int [B]^T [D] [B] d(\text{vol}) \quad (7)$$

$[K_e]$ is the stiffness matrix of element e

$$[R_e] = \int [N]^T [X_e] d(\text{surf}) \quad (8)$$

$[R_e]$ is the generalized load vector

$[X_e]$ is the surface traction vector

and the matrices $[N]$, $[B]$ and $[D]$ are defined by the equations

$$[\omega] = [uv]^T = [N][\omega_e] \quad (9)$$

$$[\epsilon] = [\epsilon_x \epsilon_y \gamma_{xy}]^T = [B][\omega] \quad (10)$$

$$[\sigma] = [\sigma_x \sigma_y \tau_{xy}]^T = [D][\epsilon] . \quad (11)$$

For the coefficient matrix in system (4), the term "total stiffness matrix" is used. This matrix is formed by combining the stiffness matrices of the individual elements in a systematic way.

System (4) is then solved numerically for the nodal displacements $[\omega_i] = [u_i v_i]^T \quad i=1, \dots, n$. Once the nodal displacements are known, the strains and the stresses within each element can also be determined.

The solution thus obtained converges to the exact elastic solution provided that the displacement functions satisfy the following requirements

- (a) the displacement boundary conditions are satisfied
- (b) displacement continuity across element boundaries is preserved
- (c) the displacement field and its first derivatives (strains) tend to the true fields everywhere as the number of elements tends to infinity.

If triangular elements and linear displacement

functions are chosen, the resulting element type is designated as CST (constant strain triangular element). This is the most frequently used type of element, since it combines simplicity, flexibility and adequate accuracy for a wide range of applications.

3. SPECIAL FINITE ELEMENT TECHNIQUES

Early attempts to compute stress intensity factors by the method of finite elements have only met with partial success due to the presence of a mathematical singularity at the crack tip. Indeed, from equations (1), (2) and (3) it follows that the stresses become infinite as one approaches the tip ($r \rightarrow 0$). Since for elastic bodies the strains are linear functions of the stresses, it follows that they also become unbounded.

The same conclusion can be reached from the equations describing the displacement field associated with the crack tip. They are:

$$u = \frac{K_I}{\mu} \left(\frac{r}{2\pi}\right)^{\frac{1}{2}} \cos\frac{\theta}{2} [1 - 2h + (\sin\frac{\theta}{2})^2] \\ + \frac{K_{II}}{\mu} \left(\frac{r}{2\pi}\right)^{\frac{1}{2}} \sin\frac{\theta}{2} [2 - 2h + (\cos\frac{\theta}{2})^2] \quad (12)$$

$$v = \frac{K_I}{\mu} \left(\frac{r}{2\pi}\right)^{\frac{1}{2}} \sin\frac{\theta}{2} [2 - 2h - (\cos\frac{\theta}{2})^2] \\ + \frac{K_{II}}{\mu} \left(\frac{r}{2\pi}\right)^{\frac{1}{2}} \cos\frac{\theta}{2} [1 - 2h + (\sin\frac{\theta}{2})^2] \quad (13)$$

It is evident that the displacement derivatives (strains) contain the factor $r^{-1/2}$ which tends to infinity

for $r \rightarrow 0$.

As a result, in the vicinity of the tip, one of the basic assumptions which ensure convergence of the finite element solution to the exact elastic solution is no longer valid. This is the assumption that the approximate displacement field and its first derivatives (strains) can be made arbitrarily close to the true fields everywhere in the region by increasing the number of elements. For standard CST elements this assumption is violated since, by definition, the strain within each element is constant and as such it cannot adequately represent the true strain which increases indefinitely as one approaches the tip.

Clearly, for the method of finite elements to succeed, a more accurate representation of the displacement field around the tip is needed. This line of reasoning led investigators to combine a special element (or elements) covering the vicinity of the tip, with standard CST elements covering the rest of the body. For the special element a pair of displacement functions is chosen which provides a more accurate representation of the tip singularity.

Depending on the choice of displacement functions and the shape of the special element several variations of this basic technique are possible and some of them have yet to be explored. Those which were investigated so far, however,

succeeded in determining stress intensity factors with sufficient accuracy. Moreover, numerical procedures are now available for the construction of the total stiffness matrix and these can be utilized for the development of more powerful techniques.

4. WILSON'S METHOD

In order to illustrate the idea of combining a special element with standard CST elements, a specific technique will be described which is due to W. K. Wilson [4] and uses a circular element centered at the crack tip.

One important consideration is the choice of appropriate displacement functions to be used in connection with this element. Initially, Wilson [2] and Hilton and Hutchinson [3] utilized the asymptotic equations (12) and (13) which perhaps is a natural choice. For a special element of this type they found that sufficient accuracy is obtained if the diameter of the circular element is less than 2% of the crack length. This means that a highly refined element representation is required around the crack tip for adequate estimates of the intensity factor. For geometrically complex bodies or for bodies containing more than one crack, the total number of elements required may outgrow the memory capacity of normally available computer facilities.

The necessity of using a small circular element is caused by the fact that the accuracy of the approximate displacement functions (12) and (13) deteriorates rapidly as one moves away from the tip. In fact, each of these functions contains only the leading terms of an asymptotic

expansion. Hence, an improvement in accuracy can be expected if a few higher order terms are retained in the expansion.

Such an improved technique was developed by Wilson [4]. The displacement field within the circular element is represented by the following functions

$$u = \sum_{k=1}^4 \left(\frac{r}{r_c}\right)^{k/2} f_k(\theta) \delta_k \quad (14)$$

$$v = \sum_{k=1}^4 \left(\frac{r}{r_c}\right)^{k/2} g_k(\theta) \delta_k \quad (15)$$

$$\text{where } f_k(\theta) = F_k(\theta) \cos \theta - G_k(\theta) \sin \theta \quad (16)$$

$$g_k(\theta) = F_k(\theta) \sin \theta + G_k(\theta) \cos \theta \quad (17)$$

$$F_1(\theta) = - \left(\frac{5}{2} - 4h\right) \cos \frac{\theta}{2} + \frac{1}{2} \cos \frac{3\theta}{2}$$

$$F_2(\theta) = (2 - 4h) + 2 \cos 2\theta$$

$$F_3(\theta) = \left(\frac{3}{2} - 4h\right) \cos \frac{\theta}{2} + \frac{1}{2} \cos \frac{5\theta}{2}$$

$$F_4(\theta) = - (1 - 4h) \cos \theta - 3 \cos 3\theta$$

$$G_1(\theta) = \left(\frac{7}{2} - 4h\right) \sin \frac{\theta}{2} - \frac{1}{2} \sin \frac{3\theta}{2}$$

$$G_2(\theta) = - 2 \sin 2\theta$$

$$G_3(\theta) = \left(\frac{9}{2} - 4h\right) \sin \frac{\theta}{2} - \frac{1}{2} \sin \frac{5\theta}{2}$$

$$G_4(\theta) = - (5 - 4h) \sin \theta + 3 \sin 3\theta$$

r_c is the radius of the circular element and δ_j ($j=1, \dots, 4$) are unknown parameters.

As explained in Wilson's paper, the four terms in each displacement component correspond to the first four symmetric terms of the William's stress function. It must be pointed out that since only symmetric terms are used, the displacement functions defined by (14) and (15) are applicable only to a mode I type of stress field. The resulting high order circular element is designated as SSC-4.

The stiffness matrix of the SSC-4 element with respect to the vector $[\delta_c] = [\delta_1 \delta_2 \delta_3 \delta_4]^T$ is obtained from equation (7). This is a symmetric four by four matrix and its elements are

$$a_{11} = \mu(\pi/2)(5 - 8h)$$

$$a_{12} = \mu(64/15)(-2 + 5h)$$

$$a_{13} = \mu(3\pi)(-1 + 2h)$$

$$a_{14} = \mu(128/105)(6 - 7h)$$

$$a_{22} = \mu(16\pi)(1 - h)$$

$$a_{23} = \mu(64/5)(2 - 3h)$$

$$a_{24} = 0$$

$$a_{33} = \mu(\pi/2)(15 - 24h)$$

$$a_{3,4} = \mu(128/35)(-6 + 5h)$$

$$a_{4,4} = \mu(16\pi)(3 - h) .$$

The advantage of the SSC-4 element lies in the fact that the approximate displacement functions (14) and (15) provide adequate accuracy over a larger area around the crack tip. Hence, a larger SSC-4 element and a less refined triangular representation around it may be used and, as a result, significant savings in computer memory and processing time can be realized.

4.1 CONSTRUCTION OF THE TOTAL STIFFNESS MATRIX

For a finite element representation consisting of a high order circular crack tip element (SSC-4) and constant strain triangular elements (CST) in the rest of the region, the total stiffness matrix can be constructed in the usual way by combining the individual element stiffness matrices.

If a conventional CST program is available, however, a simpler approach may be used. First, the CST program is applied to the triangular elements only. Then, the total stiffness matrix of the combined representation is obtained by modifying the total stiffness matrix generated by the CST program. A description of this last procedure in mathematical terms is presented below.

The total potential energy of the system is the sum of the potential energy of the triangular elements and the potential energy of the circular element

$$\Pi = \Pi_t + \Pi_c . \quad (18)$$

The parameters of the system must be chosen so as to minimize Π . There are three sets of parameters. The first set includes the displacement components u_i, v_i of all nodes i ($i=1, \dots, n_1$), lying outside the circumference of the circular element. The second set includes the displacement components u_j, v_j of the nodes j ($j=1, \dots, n_2$), which are located on the circumference of the circular element. The third set contains the parameters δ_k ($k=1, \dots, 4$) of the circular element.

These parameters are, in fact, not all independent from each other. Those of the second set are related to those of the third through the equations

$$u_j = \sum_{k=1}^4 f_k(\theta_j) \delta_k \quad (19)$$

$$v_j = \sum_{k=1}^4 g_k(\theta_j) \delta_k \quad (20)$$

where θ_j is the angular position of node j , and $f_k(\theta_j)$, $g_k(\theta_j)$ are defined by equations (16) and (17).

The dependence of the potential energies Π_t and Π_c on

the system parameters is described by the following functional relationships

$$\Pi_t = \Pi_t \{u_i, v_i, u_j(\delta_k), v_j(\delta_k)\} \quad (21)$$

$$\Pi_c = \Pi_c \{u_j(\delta_k), v_j(\delta_k)\} . \quad (22)$$

The principle of minimum potential energy for the combined representation requires that the following system be satisfied

$$\frac{\partial \Pi}{\partial u_i} = 0 , \quad \frac{\partial \Pi}{\partial v_i} = 0 \quad i=1, \dots, n_1 \quad (23)$$

$$\frac{\partial \Pi}{\partial \delta_k} = 0 \quad k=1, \dots, 4 . \quad (24)$$

From (18), (21) and (22) we have

$$\frac{\partial \Pi}{\partial u_i} = \frac{\partial \Pi_t}{\partial u_i} + \frac{\partial \Pi_c}{\partial u_i} = \frac{\partial \Pi_t}{\partial u_i} \quad \left(\frac{\partial \Pi_c}{\partial u_i} = 0 \right) \quad (25)$$

$$\frac{\partial \Pi}{\partial v_i} = \frac{\partial \Pi_t}{\partial v_i} + \frac{\partial \Pi_c}{\partial v_i} = \frac{\partial \Pi_t}{\partial v_i} \quad \left(\frac{\partial \Pi_c}{\partial v_i} = 0 \right) \quad (26)$$

$$\frac{\partial \Pi}{\partial \delta_k} = \frac{\partial \Pi_t}{\partial \delta_k} + \frac{\partial \Pi_c}{\partial \delta_k} ; \quad (27)$$

hence, equations (23) and (24) may be written

$$\frac{\partial \Pi_t}{\partial u_i} = 0 , \quad \frac{\partial \Pi_t}{\partial v_i} = 0 \quad i=1, \dots, n_1 \quad (28)$$

$$\frac{\partial \Pi}{\partial \delta_k} = \frac{\partial \Pi_t}{\partial \delta_k} + \frac{\partial \Pi_c}{\partial \delta_k} = 0 \quad k=1, \dots, 4 . \quad (29)$$

Let us now neglect the presence of the circular element and develop a system of equations for the triangular elements only

$$\frac{\partial \Pi_t}{\partial u_i} = 0, \quad \frac{\partial \Pi_t}{\partial v_i} = 0 \quad i=1, \dots, n_1 \quad (30)$$

$$\frac{\partial \Pi_t}{\partial u_j} = 0, \quad \frac{\partial \Pi_t}{\partial v_j} = 0 \quad j=1, \dots, n_2 \quad (31)$$

It is apparent that this system results from the application of a conventional finite element program on the triangular elements only.

The desired system of equations (28) and (29) is derived by applying the following two operations on equations (30) and (31):

- (1) all u_j and v_j in equations (30) and (31) are substituted by the right-hand sides of equations (19) and (20). At the end of this operation equations (28) and (30) will be identical.
- (2) In view of the functional relationship (21), equations (29) may be written

$$\frac{\partial \Pi}{\partial \delta_k} = \frac{\partial \Pi_c}{\partial \delta_k} + \sum_{j=1}^{n_2} \left[\frac{\partial \Pi_t}{\partial u_j} \frac{\partial u_j}{\partial \delta_k} + \frac{\partial \Pi_t}{\partial v_j} \frac{\partial v_j}{\partial \delta_k} \right] \quad k=1, \dots, 4 \quad (32)$$

From (19) and (20) we have

$$\frac{\partial u_j}{\partial \delta_k} = f_k(\theta_j) \quad (33)$$

$$\frac{\partial v_j}{\partial \delta_k} = g_k(\theta_j) \quad (34)$$

Moreover, let $[\delta_c] = [\delta_1 \delta_2 \delta_3 \delta_4]^T$ and also let $[A] = [a_{ij}]$ be the 4×4 stiffness matrix of the circular element. Then

$$\frac{\partial \Pi_c}{\partial [\delta_c]} = [A][\delta_c] \quad (35)$$

from which

$$\frac{\partial \Pi_c}{\partial \delta_k} = a_{1k} \delta_1 + a_{2k} \delta_2 + a_{3k} \delta_3 + a_{4k} \delta_4 = \sum_{\ell=1}^4 a_{\ell k} \delta_\ell \quad (36)$$

With these developments equations (32) become

$$\frac{\partial \Pi}{\partial \delta_k} = \sum_{\ell=1}^4 a_{\ell k} \delta_\ell + \sum_{j=1}^{n_2} \left[\frac{\partial \Pi_t}{\partial u_j} f_k(\theta_j) + \frac{\partial \Pi_t}{\partial v_j} g_k(\theta_j) \right] \quad k=1, \dots, 4 \quad (37)$$

Equation (37) defines the second operation that must be performed on the left-hand sides $\partial \Pi_t / \partial u_j$ and $\partial \Pi_t / \partial v_j$ of equations (31) in order to obtain the left-hand sides of equations (29).

4.2 MATRIX FORMULATION

Wilson's method as described above was then implemented. Utilizing a conventional CST finite element program written

by E. L. Wilson* [5] as a starting point, a computer program was developed for the calculation of the mode I stress intensity factor.

A basic feature of E. L. Wilson's program lies in the fact that, as system parameters serve the vectors, $[\omega_j] = [u_j, v_j]^T$ rather than the individual displacement components u_j, v_j . As a result, the elements of the total stiffness matrix generated by this program are 2×2 submatrices.

We will now present a formulation of Wilson's method which is specially adapted to this particular CST program. In place of the four circular element parameters $\delta_1, \delta_2, \delta_3$ and δ_4 we introduce the vector parameters $[\delta_I] = [\delta_1, \delta_2]^T$ and $[\delta_{II}] = [\delta_3, \delta_4]^T$. Equations (19) and (20) become

$$[\omega_j] = \begin{bmatrix} f_{j1} & f_{j2} \\ g_{j1} & g_{j2} \end{bmatrix} [\delta_I] + \begin{bmatrix} f_{j3} & f_{j4} \\ g_{j3} & g_{j4} \end{bmatrix} [\delta_{II}] \quad (38)$$

The system of equations for the triangular elements (equations (30) and (31)) may be written

$$\frac{\partial \Pi_t}{\partial [\omega_i]} = 0 \quad i=1, \dots, n_1 \quad (39)$$

$$\frac{\partial \Pi_t}{\partial [\omega_j]} = 0 \quad j=1, \dots, n_2 \quad (40)$$

*not to be confused with W. K. Wilson, the author of the method being described.

Also, equations (37) may be written in matrix form as follows

$$\frac{\partial \Pi}{\partial [\delta_I]} = \begin{bmatrix} a_{11} & a_{12} \\ a_{21} & a_{22} \end{bmatrix} [\delta_I] + \begin{bmatrix} a_{13} & a_{14} \\ a_{23} & a_{24} \end{bmatrix} [\delta_{II}] + \sum_{j=1}^{n_2} \begin{bmatrix} f_{j1} & f_{j2} \\ g_{j1} & g_{j2} \end{bmatrix}^T \frac{\partial \Pi_t}{\partial [\omega_j]} \quad (41)$$

$$\frac{\partial \Pi}{\partial [\delta_{II}]} = \begin{bmatrix} a_{31} & a_{32} \\ a_{41} & a_{42} \end{bmatrix} [\delta_I] + \begin{bmatrix} a_{33} & a_{34} \\ a_{43} & a_{44} \end{bmatrix} [\delta_{II}] + \sum_{j=1}^{n_2} \begin{bmatrix} f_{j3} & f_{j4} \\ g_{j3} & g_{j4} \end{bmatrix}^T \frac{\partial \Pi_t}{\partial [\omega_j]} \quad (42)$$

The system of equations for the combined representation (equations (28) and (29)) becomes

$$\frac{\partial \Pi_t}{\partial [\omega_j]} = 0 \quad i=1, \dots, n_1 \quad (43)$$

$$\frac{\partial \Pi}{\partial [\delta_I]} = 0, \quad \frac{\partial \Pi}{\partial [\delta_{II}]} = 0. \quad (44)$$

This system is obtained by applying the following two operations on equations (39) and (40):

- (1) for all $[\omega_j]$ in equations (39) and (40) the substitution defined by equation (38) is made. At the end of

this operation, equations (39) and (43) are identical.

- (2) the left-hand sides of equations (44) are derived by combining the left-hand sides of equations (40) according to equations (41) and (42).

4.3 DISPLACEMENT OF THE CRACK TIP

The displacement components at any given point (r, θ) within the circular element, as defined by equations (14) and (15), are in fact relative displacements with respect to the crack tip. For $r=0$ (crack tip), both displacement components become equal to zero. Thus, in effect, equations (14) and (15) do not allow any movement of the crack tip.

In practice, however, the crack tip may not be a fixed point, as, for example, in the strip problem to be investigated. From physical considerations it is apparent that, as a result of the tensile load, the crack tip is horizontally displaced (Figure 1).

It then becomes necessary to modify the mathematical model of the system, so that displacements of the crack tip are permitted. This is done by introducing the displacement vector of the crack tip $[\omega_t] = [u_t v_t]^T$ as an additional parameter and writing equation (38) in the form

$$[\omega_j] = \begin{bmatrix} f_{j1} & f_{j2} \\ g_{j1} & g_{j2} \end{bmatrix} [\delta_I] + \begin{bmatrix} f_{j3} & f_{j4} \\ g_{j3} & g_{j4} \end{bmatrix} [\delta_{II}] + \begin{bmatrix} 1 & 0 \\ 0 & 1 \end{bmatrix} [\omega_t] . \quad (45)$$

The parameters of the system are determined by solving the linear system

$$\frac{\partial \Pi_t}{\partial [\omega_j]} = 0 \quad i=1, \dots, n_1 \quad (46)$$

$$\frac{\partial \Pi}{\partial [\delta_I]} = 0 , \quad \frac{\partial \Pi}{\partial [\delta_{II}]} = 0 , \quad \frac{\partial \Pi}{\partial [\omega_t]} = 0 . \quad (47)$$

The left-hand side of the additional equation

$$\frac{\partial \Pi}{\partial [\omega_t]} = 0$$

is obtained by combining the left-hand sides of equations (40) according to

$$\frac{\partial \Pi}{\partial [\omega_t]} = \sum_{j=1}^{n_2} \begin{bmatrix} 1 & 0 \\ 0 & 1 \end{bmatrix} \frac{\partial \Pi_t}{\partial [\omega_j]} . \quad (48)$$

Otherwise, the procedure for deriving equations (46) and (47) is exactly the same.

4.4 CALCULATION OF THE MODE I STRESS INTENSITY FACTOR

The mode I stress intensity factor K_I is directly related to the crack tip element parameter δ_1 . This is only natural since K_I is the constant coefficient of the first

term in equation (12), δ_1 is the constant coefficient of the first term in equation (14) and both these equations are two different truncated forms of the same asymptotic expansion.

In order to derive this relationship let us develop the first term of equation (14). We have

$$\begin{aligned} \delta_1 \left(\frac{r}{r_c}\right)^{1/2} f_1(\theta) &= \delta_1 \left(\frac{r}{r_c}\right)^{1/2} \left\{ \left[-\left(\frac{5}{2} - 4h\right) \cos\frac{\theta}{2} + \frac{1}{2} \cos\frac{3\theta}{2} \right] \cos\theta \right. \\ &\quad \left. - \left[\left(\frac{7}{2} - 4h\right) \sin\frac{\theta}{2} - \frac{1}{2} \sin\frac{3\theta}{2} \right] \sin\theta \right\} \end{aligned}$$

and after some algebra

$$\delta_1 \left(\frac{r}{r_c}\right)^{1/2} f_1(\theta) = -2\delta_1 \left(\frac{r}{r_c}\right)^{1/2} \cos\frac{\theta}{2} \left[1 - 2h + \left(\sin\frac{\theta}{2}\right)^2 \right].$$

Comparing this result with the first term of equation (12) we see that they are the same if

$$-2\delta_1 \left(\frac{r}{r_c}\right)^{1/2} = \frac{K_I}{\mu} \left(\frac{r}{2\pi}\right)^{1/2}$$

from which

$$K_I = -\mu \left(\frac{8\pi}{r_c}\right)^{1/2} \delta_1. \quad (49)$$

The procedure for computing K_I may now be summarized as follows:

- (1) A finite element representation is prepared for the cracked body consisting of one circular SSC-4 element

centered at each crack tip and triangular CST elements everywhere else in the region.

- (2) Data cards describing this representation are prepared and read by the computer program.
- (3) For the adopted representation the program develops first the linear system of equations (39) and (40) and then the linear system of equations (46) and (47).
- (4) The system of equations (46) and (47) is solved and the values of the parameters δ_i ($i=1, \dots, 4$) of each crack tip element are determined.
- (5) Using the computed value of δ_1 at each crack tip, the mode I stress intensity factor K_I is calculated from equation (49).

5. APPLICATION TO A CRACKED STRIP UNDER TENSION

The effectiveness of Wilson's method was demonstrated in the case of an infinitely long strip under tension with a line crack perpendicular to its axis of symmetry (Figure 1). The method was used to investigate the influence of circular inclusions of different material properties on the stress intensity factor. This information is of considerable practical significance. In practice, such inclusions may actually be defects in an otherwise homogeneous material or fibers in a fiber-reinforced material.

For simplicity, two identical inclusions centered on the extension of the crack line and symmetrically located with respect to the crack were assumed to be present. On account of symmetry, only one fourth of the strip area was considered.

All numerical calculations were based on the following loading and geometric conditions (Figure 1)

$$\sigma = 20,000 \text{ psi}$$

$$c = 5 \text{ in}$$

$$d = 25 \text{ in}$$

The finite element layout is illustrated in Figures 2 and 3. It may be noted that most of the nodes lie on

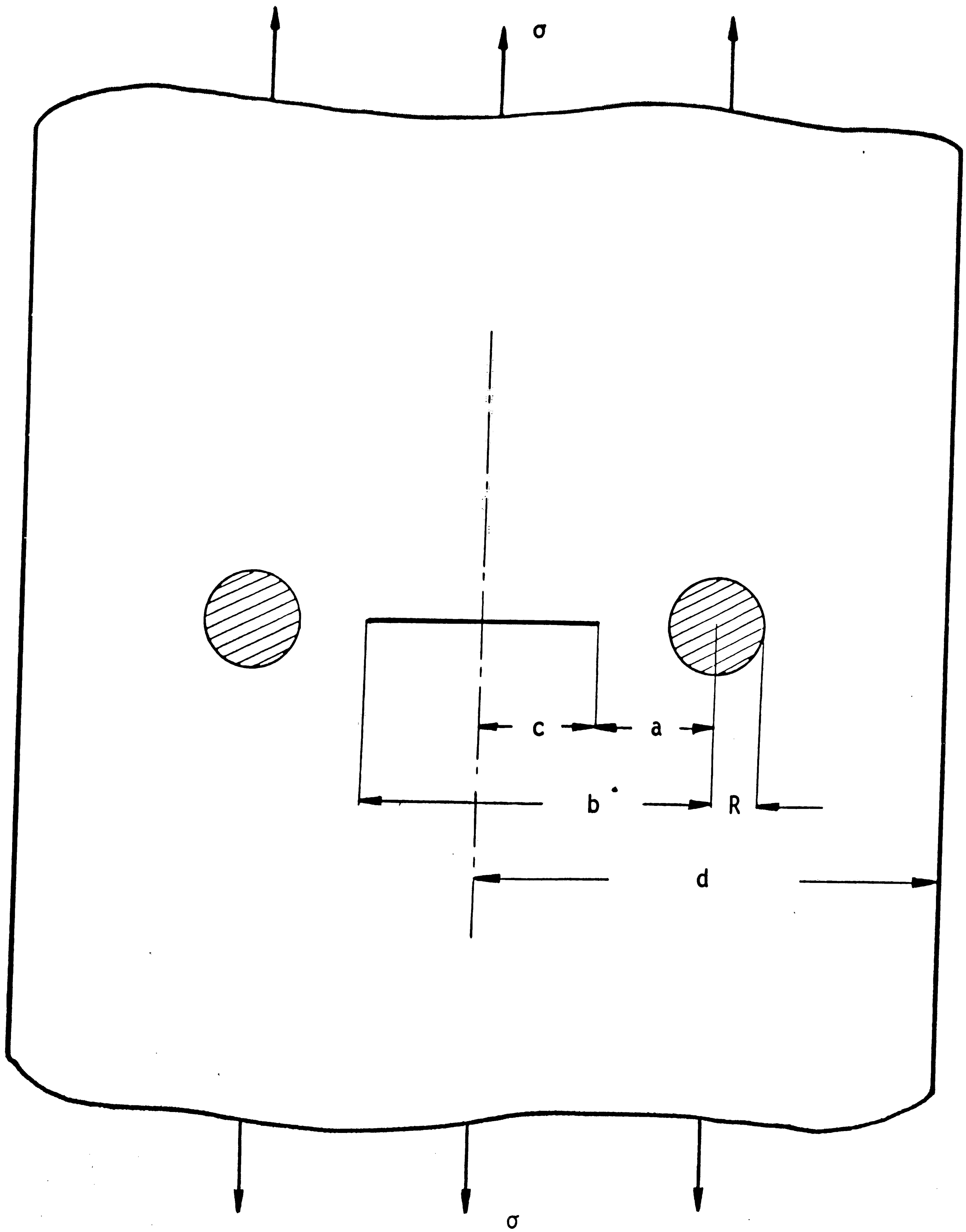


Figure 1. Infinitely long cracked strip under tension with inclusions.

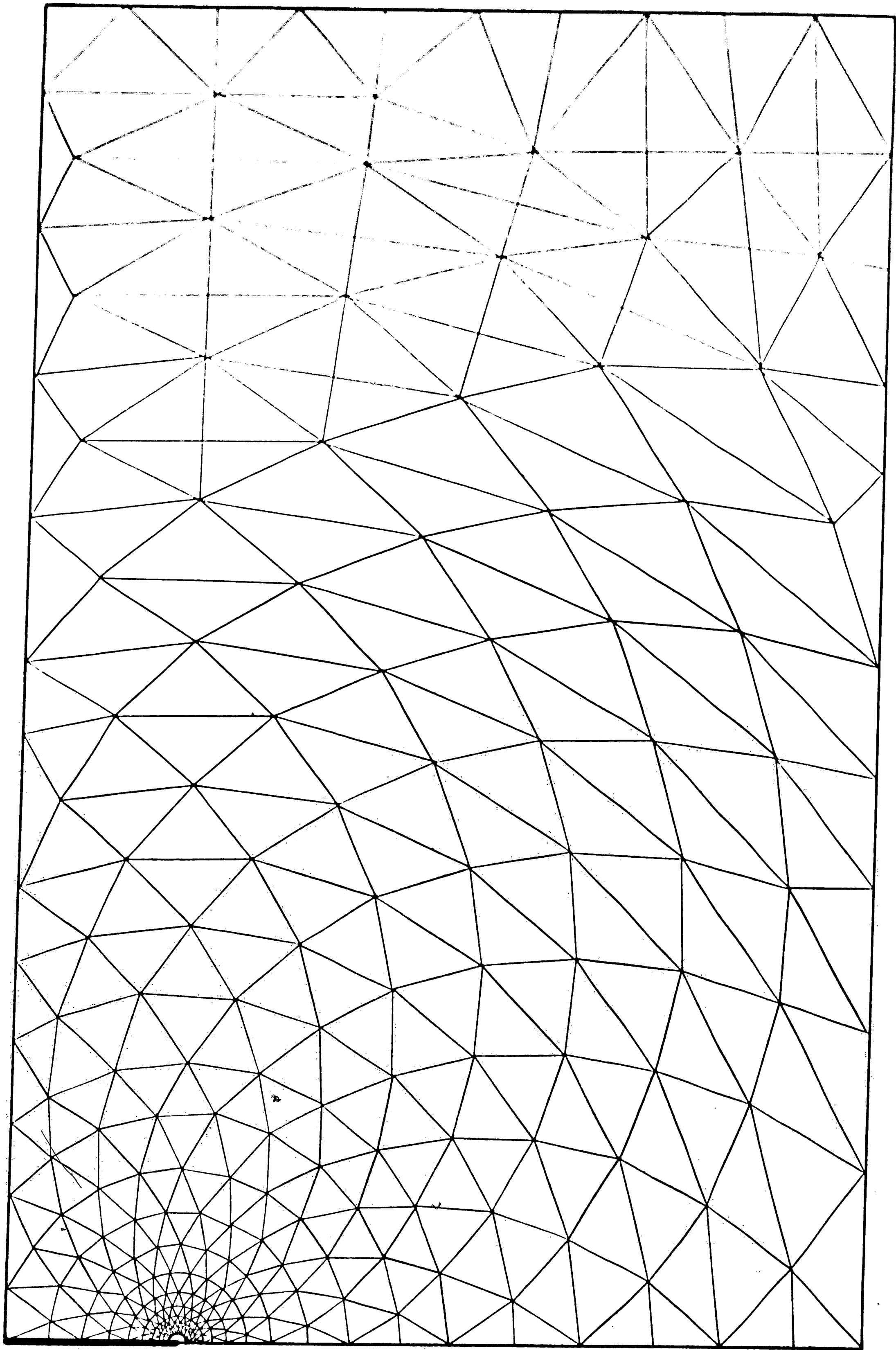


Figure 2. Finite element layout of one fourth of the strip area.

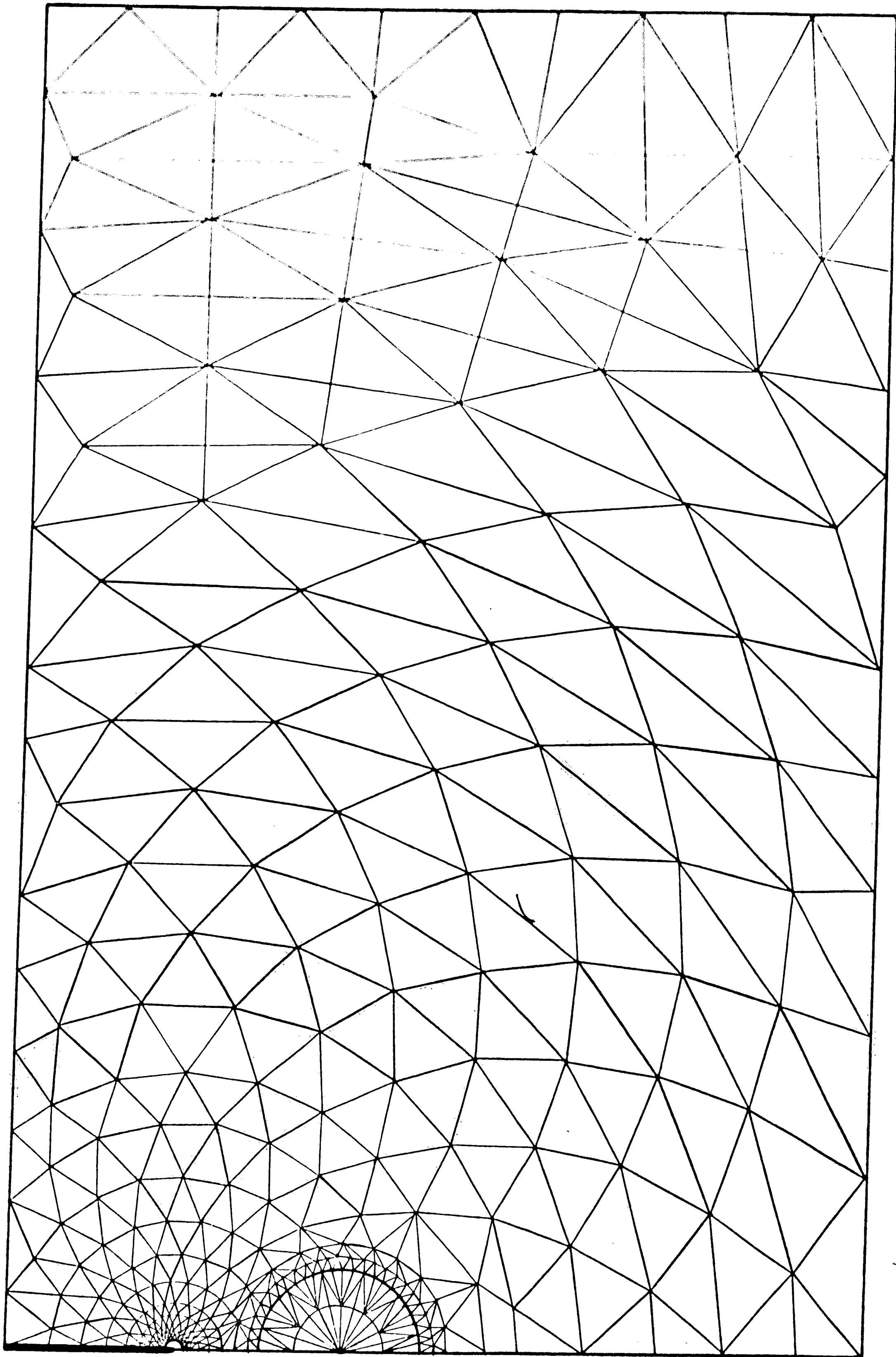


Figure 3. Typical finite element layout with inclusion.

concentric circumferences centered either at the crack tip or at the center of the inclusion. By utilizing this property, simple computer programs were created and used to generate the bulk of the data cards for the finite element program on the computer. Thus, a great deal of time was saved considering the great number of cards needed to describe the finite element patterns arising from all different positions and sizes of the inclusion.

5.1 EVALUATION OF THE METHOD'S ACCURACY

The accuracy of the method was determined by applying it to the case where no inclusion or - which is the same - inclusions of the same material properties exist. According to analytical results obtained by Isida [6], the stress intensity factor in this case is

$$K_I = \sigma(\pi c)^{1/2} f(\lambda) \quad (50)$$

where $f(\lambda)$ is a correction factor determined from Table 1.

$\lambda=c/d$	$f(\lambda)$
0.074	1.00
0.207	1.03
0.275	1.05
0.337	1.09
0.410	1.13
0.466	1.18
0.535	1.25
0.592	1.33

Table 1. Correction factor $f(\lambda)$ (equation (50)).

For the adopted loading and geometric conditions, equation (50) gives

$$K_I = 81565 \text{ psi}\cdot\text{in}^{1/2} .$$

In order to realize a certain level of accuracy, some numerical experimentation is always needed to determine the necessary degree of refinement in the finite element representation around the crack tip. For a circular element radius $r_c = 0.4$ in and number of nodes on its semicircumference $N = 25$ (Figure 4), the numerical value of the stress intensity factor was found to be $K_I = 84531 \text{ psi}\cdot\text{in}^{1/2}$ (error 3.5%). For $r_c = 0.3$ in and $N = 49$ (Figure 5), the numerical value was $K_I = 81095 \text{ psi}\cdot\text{in}^{1/2}$ (error 0.57%). This last error is very small and, therefore, further decrease in r_c or increase in N was considered unnecessary.

5.2 INFLUENCE OF INCLUSIONS ON THE INTENSITY FACTOR

The stress intensity factor is obviously affected by the presence of inclusions of different material properties in the vicinity of the crack tip. From analytical investigations on a similar problem involving an infinite sheet carried out by Tamate [7] and Sih, Hilton and Wei [8], it has been established that the geometric parameters in this relationship are the ratios b/a and R/a (Figure 1). It is reasonable to assume that the same parameters also exist in

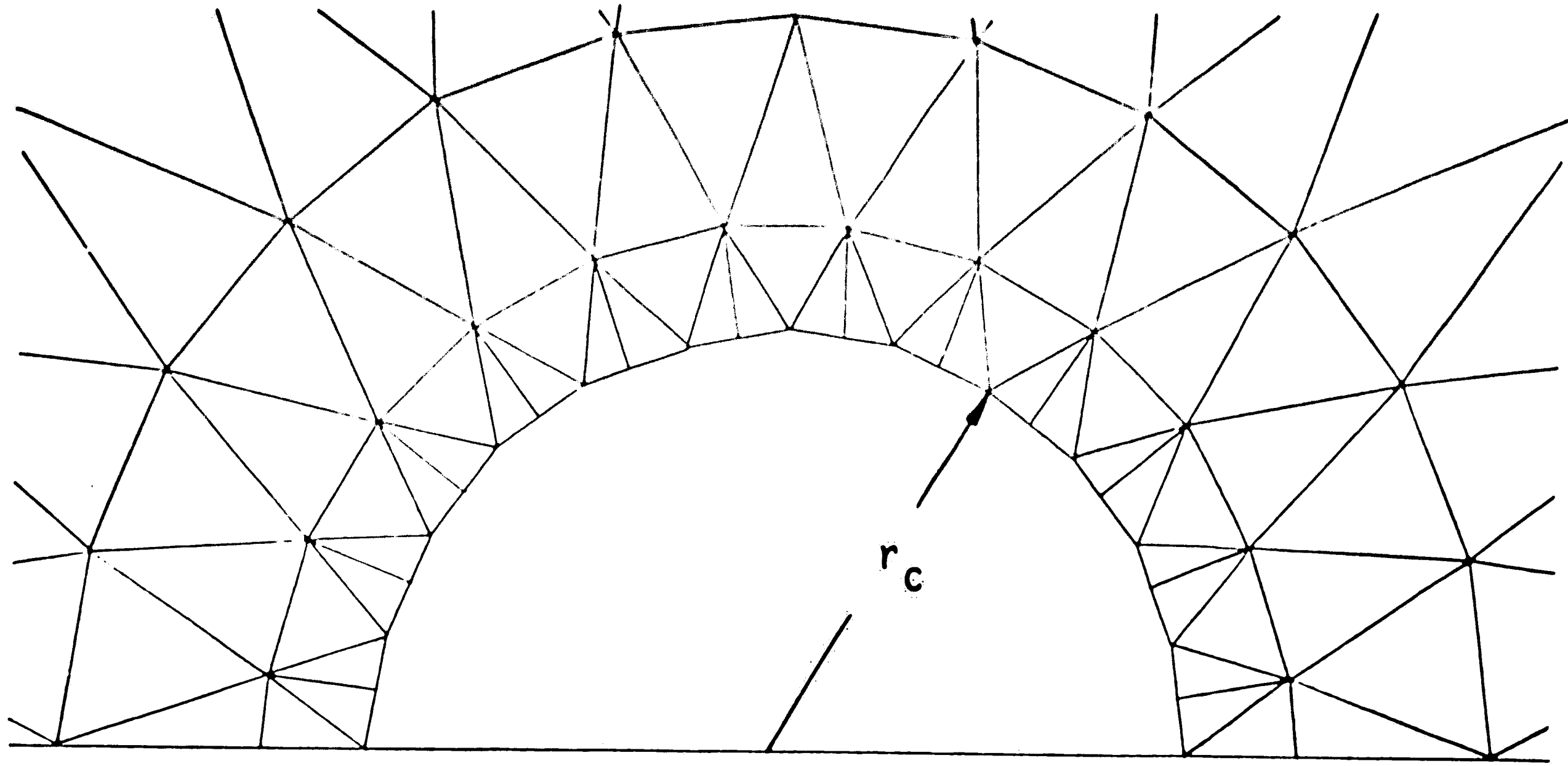


Figure 4. Element pattern around the crack tip with $r_c = 0.4$ in and $N = 25$.

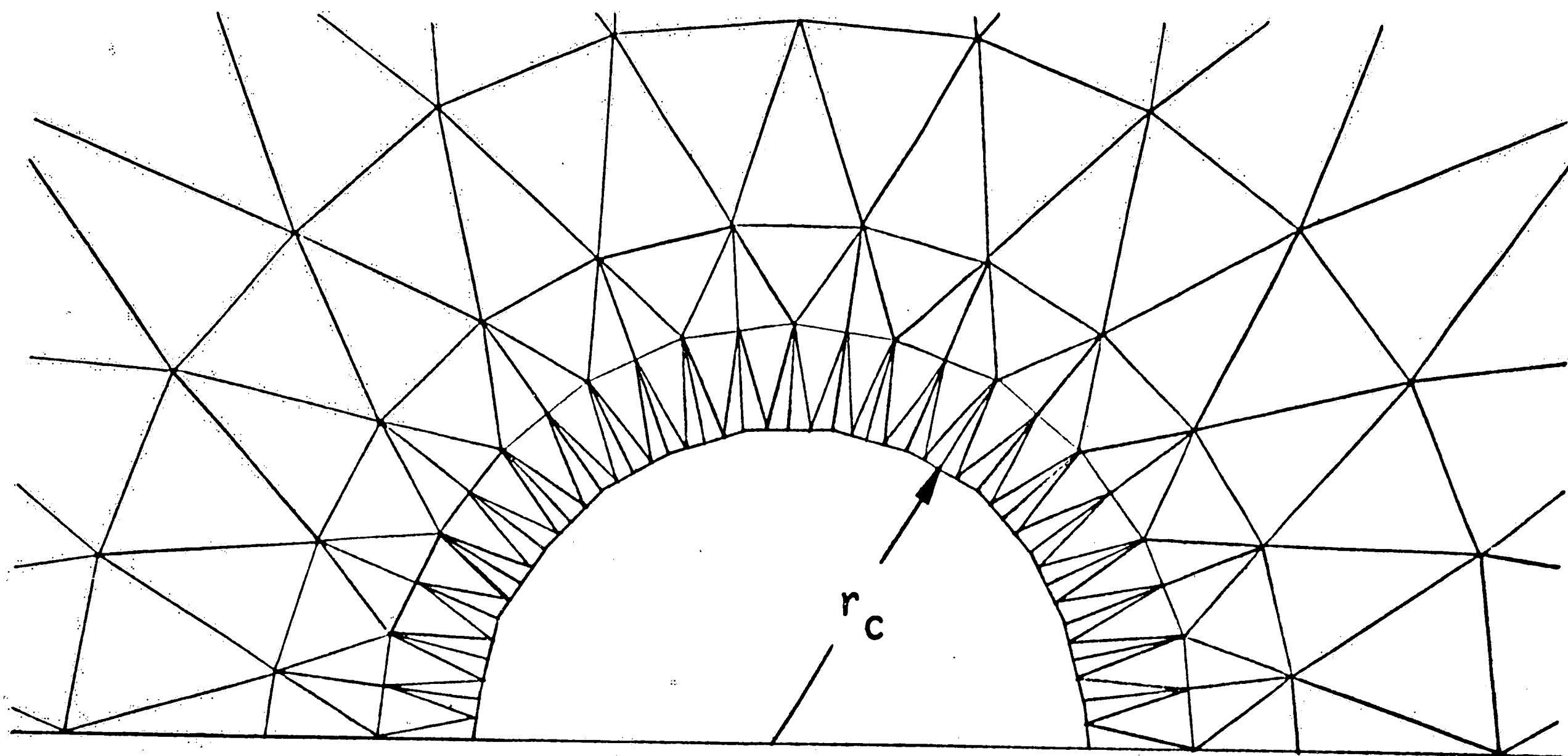


Figure 5. Element pattern around the crack tip with $r_c = 0.3$ in and $N = 49$.

the case of a strip.

The results of the numerical calculations for the strip are shown in Tables 2, 3 and 4. For each pair of values of the geometric parameters, a sufficiently refined element pattern was constructed within and around the inclusion and integrated with the overall pattern of the strip (Figure 3). For each pattern, the program was run for seven different values of the shear modulus ratio: $\mu_i/\mu = 0, 0.3, 0.6, 1.4, 2.0, 3.0, \infty$. The first value corresponds to a hole and the last one to a fixed inclusion.

In Figures 6, 7 and 8 the normalized stress intensity factor, i.e., the ratio of the stress intensity factor with inclusions to the stress intensity factor without inclusions was plotted versus the shear modulus ratio μ_i/μ .

Some approximate analytical results obtained by Sih, Hilton and Wei [8] for the case of an infinite sheet are also shown in Figure 6 for comparison.

It may be noted that in both cases the presence of a more flexible inclusion ($\mu_i < \mu$) increases the stress intensity factor, while a more rigid inclusion ($\mu_i > \mu$) decreases it. Moreover, in the case of a strip the effect of the inclusion is more pronounced. Thus, for example, a hole with a radius of 5 in ($R/a = 0.5$) increases the stress intensity factor by 49% in the case of a strip but only by 11% in the case of an infinite sheet.

$b/a = 2.0, d = 25 \text{ in}$

μ_i/μ	$R/a = 0.7$	$R/a = 0.5$	$R/a = 0.3$
0.0	184,952	121,541	92,755
0.3	119,393	97,454	86,422
0.6	95,827	87,744	83,363
1.4	72,524	77,317	79,819
2.0	65,406	73,940	78,589
3.0	59,151	70,875	77,419
∞	54,289	68,432	76,209

Table 2. Stress Intensity Factor K in $\text{psi in}^{1/2}$ versus the Shear Modulus Ratio μ_i/μ for various values of R/a , $b/a=2.0$, $d=25\text{in}$.

$b/a = 3.0, d = 25 \text{ in}$

μ_i/μ	$R/a = 0.7$	$R/a = 0.5$	$R/a = 0.3$
0.0	139,999	103,522	88,233
0.3	105,866	91,203	84,591
0.6	91,051	85,246	82,636
1.4	74,884	78,294	80,230
2.0	69,606	75,898	79,352
3.0	64,817	73,652	78,488
∞	62,621	72,794	77,953

Table 3. Stress Intensity Factor K in $\text{psi in}^{1/2}$ versus the Shear Modulus Ratio μ_i/μ for various values of R/a , $b/a=3.0$, $d=25\text{in}$.

$b/a = 4.0, d = 25 \text{ in}$

μ_j/μ	$R/a = 0.7$	$R/a = 0.5$	$R/a = 0.3$
0.0	130,171	103,508	87,036
0.3	102,287	91,327	84,047
0.6	89,754	85,418	82,407
1.4	75,745	78,504	80,373
2.0	71,081	76,116	79,622
3.0	66,802	73,873	78,878
∞	66,049	73,105	78,221

Table 4. Stress Intensity Factor K in $\text{psi in}^{1/2}$ versus the Shear Modulus Ratio μ_j/μ for various values of R/a , $b/a=4.0$, $d=25\text{in}$.

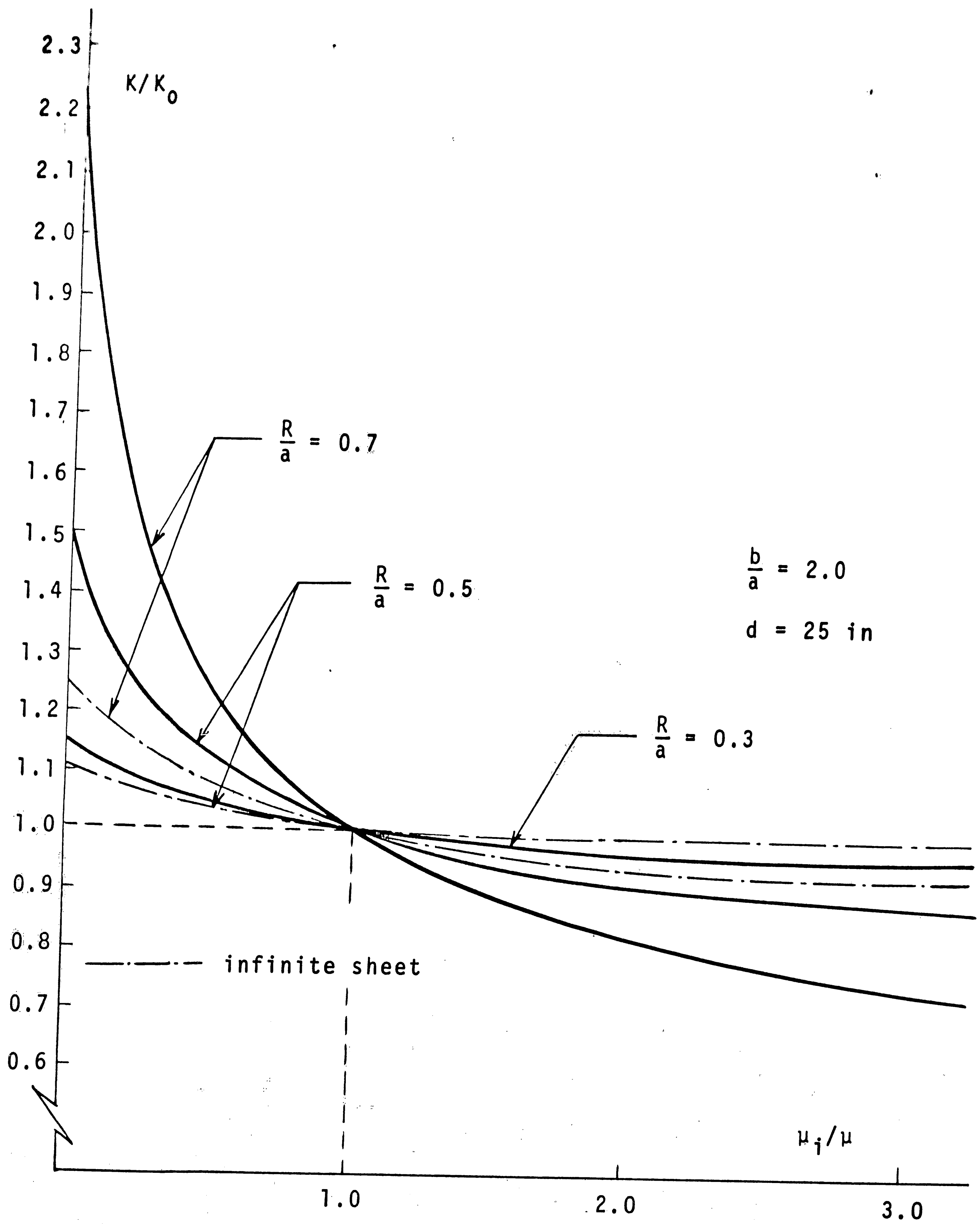


Figure 6. Normalized Stress Intensity Factor K/K_0 versus the Shear Modulus Ratio μ_i/μ for various values of R/a , $b/a = 2.0$, $d = 25$ in.

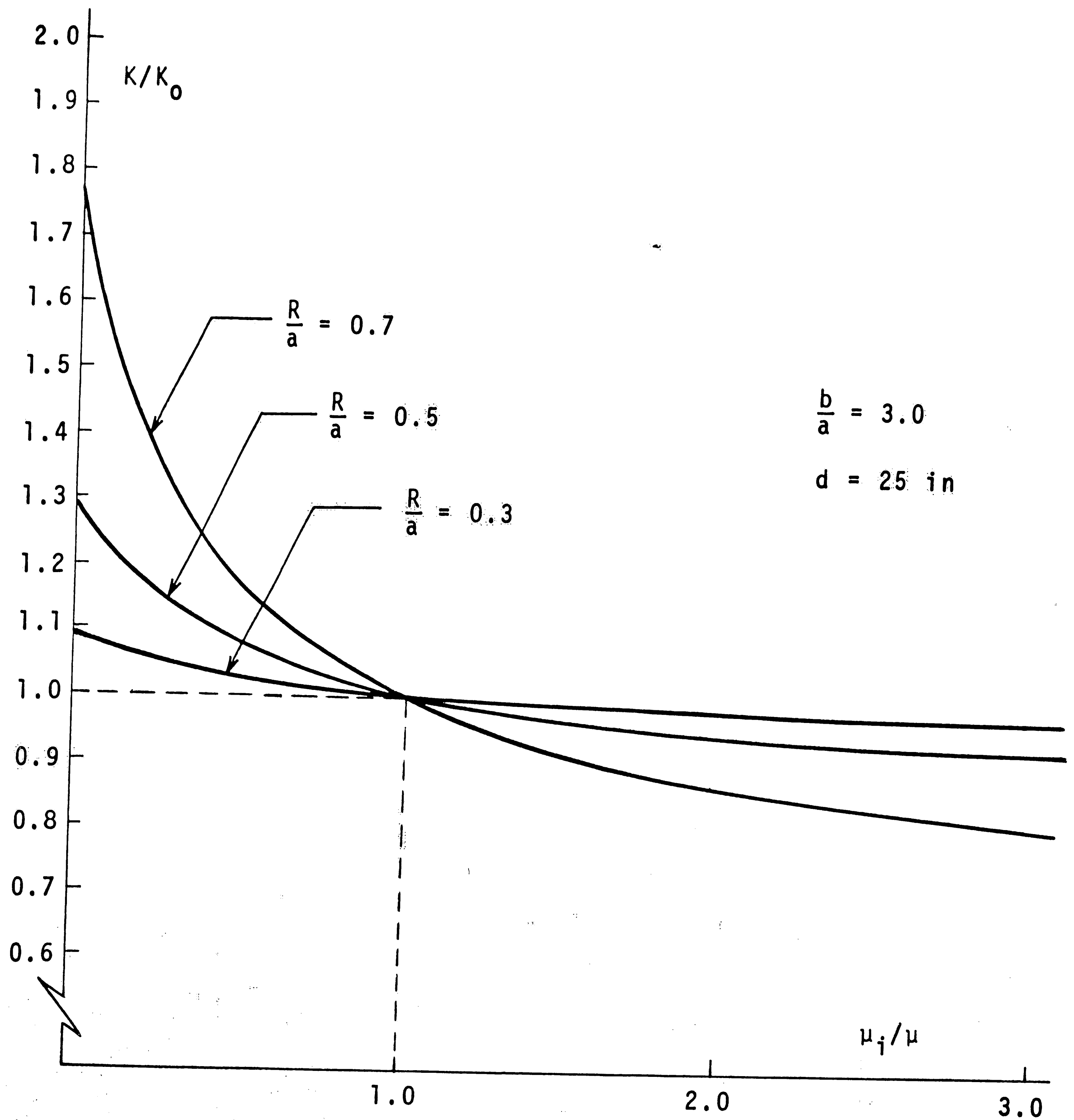


Figure 7. Normalized Stress Intensity Factor K/K_0 versus the Shear Modulus Ratio μ_i/μ for various values of R/a , $b/a = 3.0$, $d = 25 \text{ in}$.

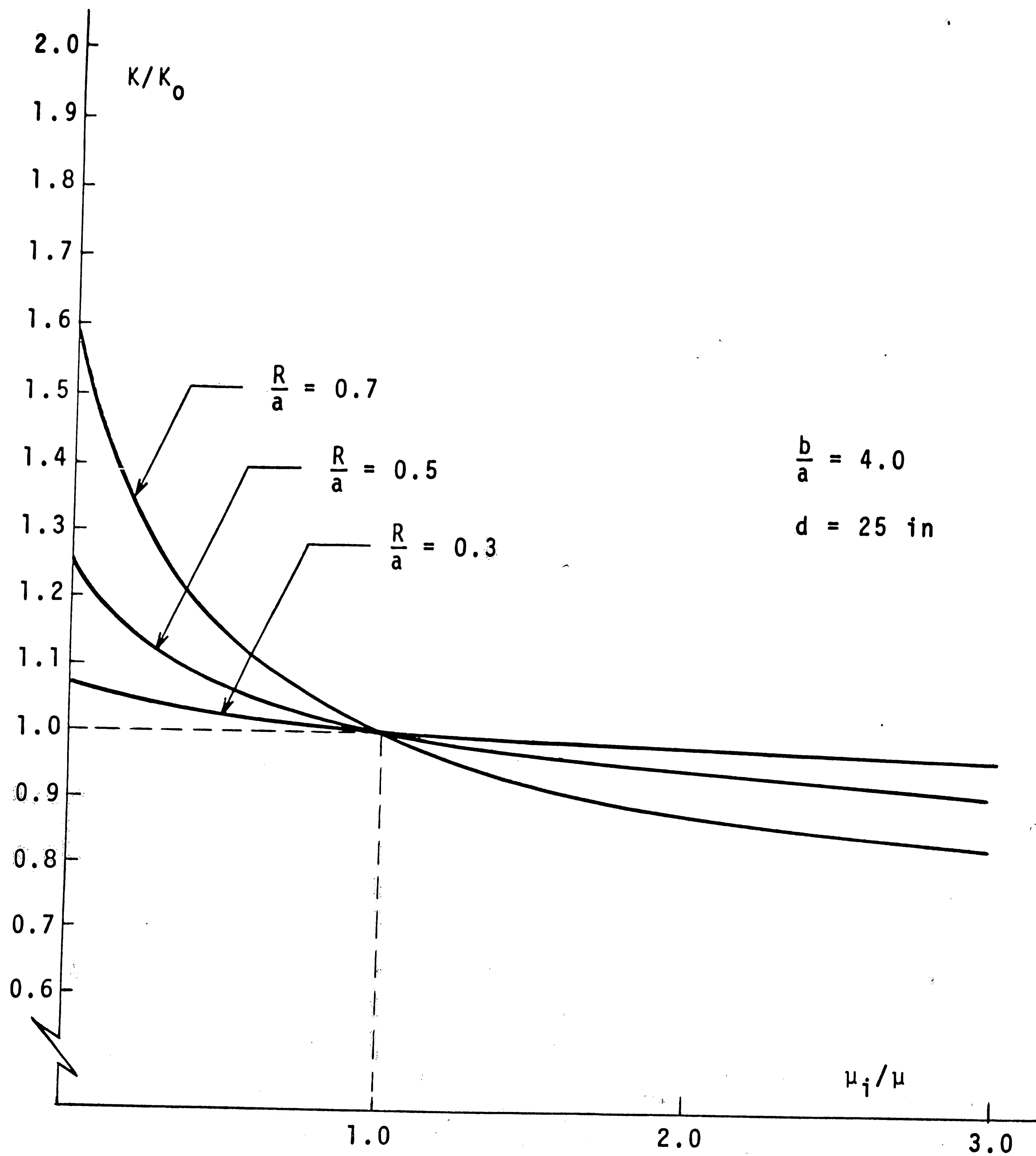


Figure 8. Normalized Stress Intensity Factor K/K_0 versus the Shear Modulus Ratio μ_i/μ for various values of R/a , $b/a = 4.0$, $d = 25$ in.

6. FINAL REMARKS

This thesis has analyzed the basic ideas which underlie the development of efficient finite element techniques for the calculation of stress intensity factors. In that respect, Wilson's method must be viewed only as a specific example of the application of these ideas. It is apparent that special elements for mode II, mode III or mixed mode stress fields can be developed in a quite analogous manner.

With respect to the strip problem, the numerical results verified the conclusions that were reached by analytical methods for an infinite sheet. Moreover, in the case of a strip, the influence of inclusions on the intensity factor was found to be stronger. Obviously, in this case, one more geometric parameter is present and this is the ratio of the strip width to the crack length. The effect of this parameter can be determined by using the same computer program.

Another interesting case arises when the inclusions are not centered on the extension of the crack line. This is a mixed mode problem, however, and its investigation would require the development of a mixed mode program.

7. COMPUTER PROGRAM

The digital computer program performs four major tasks for the analysis of a cracked structure. First, a system of linear equations for the triangular elements is formed from a basic numerical description of these elements. Second, this system is modified and transformed into a system of linear equations for the combined representation. Third, this last system is solved for the nodal displacements and the crack tip element parameters δ_1 , δ_2 , δ_3 and δ_4 . Fourth, the mode I stress intensity factor is calculated from equation (49).

The program is coded in the FORTRAN IV language and has been run on Lehigh University's CDC 6400 computer. The program is restricted to plane structures under conditions of plane stress but it can also be used for plane strain conditions if the elastic constants are modified as follows

$$E^* = \frac{E}{1-\nu^2}, \quad \nu^* = \frac{\nu}{1-\nu}$$

On a CDC 6400 computer with an available maximum net storage of 130K, structures containing as much as 750 elements and 450 nodes can be analyzed.

The input deck is prepared as follows:

A. Control card (7I4, 2E12.5, 1I1)

Cols. 1-4 Number of triangular elements
5-8 Number of nodes
9-12 Number of nodes on the semicircumference
of the circular element
13-16 Number of restrained boundary nodes
17-20 Cycle interval for the print of the force
unbalance
21-24 Cycle interval for the print of the dis-
placements and the circular element
parameters
25-28 Maximum number of cycles per run
29-40 Tolerance limit
41-52 Overrelaxation factor
53 Non-zero punch to suppress printing of
input data

B. Circular element data (F4.2, E12.5)

Cols. 1-4 Circular element radius
5-16 Young's modulus

C. Element array - 1 card per element (4X, 3I4, E12.5)

Cols. 1-4 Element number
5-8 Nodal point number i
9-12 Nodal point number j
13-16 Nodal point number k
17-28 Young's modulus

D. Nodal point array - 1 card per point (4X, 2F8.2,
2F8.0, 2F12.0)

Cols. 1-4 Nodal point number
5-12 X-ordinate
13-20 Y-ordinate
21-28 X-load
29-36 Y-load
37-48 X-displacement (initial guess)
49-60 Y-displacement (initial guess)

E. Boundary point array - 1 card per point (2I4, F8.3)

Cols. 1-4 Nodal point number
5-8 Blank if nodal point is fixed in both
directions
1 if nodal point is fixed in X-direction
2 if nodal point is free to move along a
line of slope S
9-16 Slope S (for type 2 boundary points)

Numbering rules: Both elements and nodes must be assigned consecutive integer numbers starting from 1 and placed in the input deck in the same order. The circular element need not be numbered. In addition, all nodes lying on the semicircumference of the circular element must be numbered last.

Listings of the program may be obtained from the Lehigh University Computing Center.

BIBLIOGRAPHY

- [1] Zienkiewicz, O. C. and Y. K. Cheung. The Finite Element Method in Structural and Continuum Mechanics. McGraw-Hill Inc., New York, 1967.
- [2] Wilson, W. K. Combined Mode Fracture Mechanics. University of Pittsburgh, Ph.D. Dissertation, 1969.
- [3] Hilton, P. D. and J. W. Hutchinson. Plastic Intensity Factors for Cracked Plates. Harvard University Report SM-34, May 1969.
- [4] Wilson, W. K. Crack Tip Finite Elements for Plane Elasticity. Technical Report Westinghouse Research Laboratories 71-1E7-FMPWR-P2, June 1971.
- [5] Wilson, E. L. Finite Element Analysis of Two-Dimensional Structures. Ph.D. Dissertation, University of California, Berkeley, 1963.
- [6] Isida, M. The Effect of Longitudinal Stiffeners in a Cracked Plate Under Tension. Proceedings, Fourth U.S. Congress of Applied Mechanics, 1962.
- [7] Tamate, O. The Effect of a Circular Inclusion on the Stresses Around a Line Crack in a Sheet Under Tension. International Journal of Fracture Mechanics, Vol. 4, No. 3, September 1968.
- [8] Sih, G. C., P. D. Hilton and R. P. Wei. Exploratory Development of Fracture Mechanics of Composite Systems. Air Force Technical Report AFML-TR-70-112, June 1970.

BIOGRAPHICAL NOTE

Born in Athens, Greece, on January 22, 1939, to George and Maria Papaioannou, I grew up in the city of Corinthos where I attended elementary and high school.

From 1956 to 1961 I studied Electrical and Mechanical Engineering at the National Technical University in Athens. During this period, I spent one summer with Volkswagen in Wolfsburg, W. Germany and another one with the Koninklijke Nederlandsche Hoogovens en Staalfabriken (steel and chemicals) in IJmuiden, Holland as an exchange student.

After serving 28 months in the Greek Navy with the rank of Ensign, I joined the Public Power Corporation of Greece where I supervised the construction of transmission lines and power substations from 1964 to 1967.

In January 1968 I came to the United States and from February 1968 to June 1969 I was a graduate student in Mechanical Engineering at Lehigh and a Graduate Assistant at the Lehigh University Computing Center.

Since 1968, I have done extensive work in the area of scientific computer programming. As a Graduate Assistant at Lehigh I developed a program for matrix operations (addition,

subtraction, multiplication, inversion, eigenvalues, etc.).

In August 1969 I joined the Research Development and Engineering Division of the Foxboro Company as a Systems Analyst. As a member of a group concerned with the design of a process control computer, I developed a digital logic simulation program and a program for the optimal wiring of computer back panels.

From February 1971 to April 1972 I was with the Operations Research Service of the Public Power Corporation in Athens, Greece, where I participated in the development of a program for load-flow calculations in power systems and another program for economic power dispatch.

In May 1972 I returned to the United States as an immigrant.